FCP Report No. 36

PREDICTING THE FATIGUE RESISTANCE OF WELDS

by

F. V. Lawrence, Jr., N. J. Ho and P. K. Mazumdar
Departments of Civil Engineering and Metallurgy

This report summarizes several years' work on a model for predicting the fatigue resistance of weldments. New information regarding the determination of K_t and the consequences of the $K_{f\ max}$ condition is presented. Preliminary results of the "component" weld test program are given.

A Report of the
FRACTURE CONTROL PROGRAM
College of Engineering, University of Illinois
Urbana, Illinois 61801

October, 1980

TABLE OF CONTENTS

PREDICTING THE FATIGUE RESISTANCE OF WELDS

The fatigue resistance of welds is generally less than that of the members which they join. For this reason, the fatigue resistance of weldments has been extensively studied over the years through tests on full size weldments - an expensive and time-consuming procedure. Munse (1), Gurney (2), and Sanders (3), have reviewed the results of the fatigue testing of weldments and have identified the main variables influencing their fatigue resistance. Extensive bibliographies of the literature relating to the fatigue of weldments (4-6) have been compiled. Munse and Sanders have each created computerized weldment fatigue data banks (7, 8). Others such as the British Welding Institute may also have similar resources.

The fatigue data obtained by testing often exhibit the large amount of scatter (Figure 1) two major sources of which are uncertainty as to the actual state of stress in the weldment and seemingly small variations in weld geometry. To reveal the causes of this scatter, to provide a means of interrelating the parameters which influence the fatigue life of welds, and to permit the accurate prediction of weldment fatigue resistance, an analytical model for estimating the total fatigue life of welds has been developed (9) which assumes that the total fatigue life of a weldment (N_T) is composed of a fatigue crack initiation period (N_I) and a fatigue crack propagation period (N_P) such that:

$$N_T = N_I + N_P \qquad (1)$$

The initiation portion of life (N_I) is estimated using strain-control fatigue data and is considered to consist of the number of cycles for the initiation of a fatigue crack(s) and its (their) early growth and coalescence into a dominant fatigue crack. The fatigue crack propagation portion of life (N_P) is estimated using (long-crack) fatigue-crack propagation data

assuming the "appropriate" value of the initiated crack length (a_I).

This model is quite general and can be applied to sound welds or to weld containing internal defects (10). Naturally, in the case of welds containing crack-like defects, N_I may be very short; but, for rounded internal defects such as slag or porosity, N_I may be appreciable; and, neglecting it may be excessively conservative. In some applications, lack of knowledge of the defect population of a welded structure may force one to assume the existence of an active fatigue crack immediately after fabrication and, thus, the total absence of any life devoted to fatigue crack initiation. Conversely, for welds such as production welds in machine elements, it is unlikely that serious weld defects are always present, and a major fraction of their fatigue life may be devoted to fatigue crack initiation. It is for this latter case, particularly, that the model which will be reviewed here has been developed. In its present state of development, the model is useful for predicting the fatigue resistance of weldments under constant-amplitude loadings and provide a systematic means for predicting the trend in weldment behavior when one or more of the variables influencing its fatigue resistance is altered.

THE STRESS ANALYSIS OF WELDMENTS

The first step in any fatigue analysis is to identify the location (or locations) which is the prime candidate for the initiation of a fatigue crack. A stress analysis of that region must be performed to determine (K_t) the elastic stress concentration factor (necessary for the determination of N_I) and the variation of stress along the inward path that the propagating fatigue crack will take (necessary for the determination of N_p). The finite element stress analysis method is particularly useful in this connection (Figure 2). It is important for accurate results to establish a definite weld toe radius (Figure 3) and to resolve the finite-element mesh an order of magnitude less than that radius (11).

The peak stresses at a weld toe occur in an exceedingly small region ($\simeq$ .005 in. in size Figure 3) which fact precludes their direct measurement using strain gauge or other convenient, strain-measurement methods. The peak stresses decrease rapidly with distance along the surface of the weldment away from the weld toe (y/t) and with distance inward (x/t) along the path the fatigue crack will take (Figure 4). At (y/t) of 0.3 away from the weld toe, the stresses have decreased to the level of the nominal stress in the plate (S). This fact is the basis of a useful strategy for the measurement of stresses (strains) in the vicinity of welds. Mounting a strain gauge at a distance of the plate thickness (t) away from the weld toe (or all parts of the gauge at least .3t away from the toe of the weld) will assure that the strain gauge is located as close to the weld as possible without being influenced by the stress concentration of the weld toe. Measurements of strain at this location will not depend greatly upon gauge placement and can be used in conjunction with the finite element analysis of the weld shape to determine the state of stress at the

weld toe, the elastic stress concentration factor (K_t), and the inward variation of stress along the fatigue crack path.

The elastic stress concentration factors (K_t) for several weld shapes drawn in Figure 5 are plotted versus the ratio of the plate thickness to the toe radius (t/r). The variation of $K_t - 1$ with t/r is a power function (Figure 6):

$$K_t - 1 = \alpha \, (t/r)^{\frac{1}{2}} \tag{2}$$

Because the exponent in Eq. 2 has proven to be about one-half for all case studied, it is possible to estimate K_t for any notch-root radius from a single finite-element analysis. The coefficient α is a constant which represents the macrogeometry and loading condition of the weldment. The coefficient α for bending is usually less than that for tension and, for a given joint, varies with the weld profile and the proximity of any internal defect (Table 1 also Figure 5).

Seldom are welds subjected to either pure bending or pure axial loading: most situations involve both which fact requires that welds be gauged on either side of the plate so as to determine both the axial and bending strain components. Even situations which would seem to be pure axial loading may involve considerable bending. Large induced bending stresses (S_B) may result from the straightening of a distorted weld joint under load (12).

$$S_B/\zeta = \frac{3}{4} S_A \, (L/t) \, \frac{\tanh \beta/2}{\beta/2} \; ; \; \beta = (L/t)(3S_A/E)^{\frac{1}{2}} \tag{3}$$

where: ζ is the joint distortion (radians), S_A is the induced bending stress near the weld, L is the length of weldment (ends fixed against rotation), t is the plate thickness, and E is the Young modulus. For long and slender weldments (L/t > 100), a maximum effect is achieved (Figure 5). For a steel weldment (S_A = 30 ksi, $\zeta = 1^o$, L/t > 100), a bending stress (S_B) of 14 ksi would be induced in the vicinity of the weld. It is likely that much of the scatter in fatigue data and the variability in the performance of welds is due to bending stresses which result from imperceptable joint distortions (ζ) created during fabrication. Other things being equal, this phenomenon should be less pronounced in aluminum weldments because of its lower elastic modulus.

The notch root stresses for combined axial and bending loads may be estimated using the data in Table 1 and the principle of elastic superposition:

$$\sigma = K_t^A \ S_A + K_t^B \ S_B \qquad (4)$$

where: σ is the notch root stress, $K_t^A = \alpha_A (t/r)^{\frac{1}{2}} + 1$ is the stress concentration factor for axial loads, $K_t^B = \alpha_B (t/r)^{\frac{1}{2}} + 1$ is the stress concentration factor for bending loads, α_A is the coefficient for axial loads and α_B is the coefficient for bending.

PREDICTING THE FATIGUE CRACK INITIATION LIFE (N_I)

The base metal of a weld is seldom involved in the fatigue crack initiation process (Figure 8); most fatigue cracks initiating at internal defects do so in tempered weld metal; toe cracks will initiate in the grain-coarsened heat-affected-zone (high wetting angles) or in untempered, highly diluted weld metal (low wetting angles). Thus, the fatigue properties of weld metal and HAZ are of greater relevance than those of base metal and must be determined from tests on smooth specimens (Figure 9). Test data on weld metal and heat affected zone materials are generally unavailable and difficult to obtain, experimentally (13). When test results are unavailable, it is possible to estimate roughly the fatigue strength coefficient (σ_f'), the transition fatigue life ($2N_t$), the fatigue strength exponent (b) and the mean stress relaxation exponent (k) from hardness (Figure 10) determined by measurements performed in the region which the fatigue crack is expected to initiate (13). For mild steel weldments of low hardenability, the HAZ and weld metal fatigue properties are often similar to those of base metal.

For long-life fatigue ($N_I > 10^5$ cycles), cyclic hardening and softening effects can usually be ignored, and generally elastic conditions may be assumed. For such cases, N_I can be estimated using the Basquin relationship (14):

$$\sigma_a = (\sigma_f' - \sigma_o)\ [2N_I]^b \qquad (5)$$

where: σ_a is the stress amplitude, σ_f' is the fatigue strength coefficient, σ_o is the mean stress, $2N_I$ is the reversals to fatigue crack initiation, and b is the fatigue strength exponent. The notch-root stress amplitude, the stress at the critical region in the weld (weld toe or internal defect),

can be taken as $\Delta S/2\ K_f$ so that Eq. 5 becomes:

$$\frac{\Delta S}{2} K_f = (\sigma_f' - \sigma_0) \cdot [2N_I]^b \tag{6}$$

where: ΔS is the remote stress range, and K_f is the fatigue notch factor (also K_{fmax}).

A difficulty in proceeding with the life estimation calculation suggested by Eq. 6 is determining the appropriate value of K_f for the weld toe (or for the weld defect). This difficulty arises from the fact that the notch-root radius of a discontinuity such as the weld toe is unknown and variable. Microscopic examination of weld toes reveals that practically any value of radius can be observed; thus, notches such as weld toes must be considered to have all possible values of notch-root radius which conclusion has lead to the idea of a maximum value of K_f for a given weld shape, K_{fmax} (9). K_f can be estimated using Peterson's equation (15):

$$K_f = 1 + \frac{K_t - 1}{1 + \frac{a}{r}} \tag{7}$$

where: K_t is the elastic stress concentration factor, a is a material parameter ($\simeq 10^{-3}\ (300/S_u)^2$, for steels, ksi, in. units)[1], r is the notch-root radius (in), and S_u is the ultimate strength (ksi). The elastic stress concentration factor (K_t) can be estimated using finite element

[1]The material parameter "a" is derived from long life ($\simeq 10^7$ cycles) R = -1 tests but is customarily used to predict the notch size effect for other R ratios, i.e., R = 0. The usual exponent 1.8 in the expression for "a" (for steels) has been rounded up to 2 for mathematical convenience.

methods as a function of assumed notch-root radii (r) for a given weld geometry (Figure 11). Assuming the general form of K_t suggested in Figure 6 and Eq. 2, substituting this into Eq. 7 and differentiating with respect to (r) to obtain the maximum value of K_f, K_{fmax}:

$$K_{fmax} = 1 + (\alpha/2)(t/a)^{\frac{1}{2}} \simeq 1 + .053\ \alpha\ S_u t^{\frac{1}{2}} \text{ (in steel)} \qquad (8)$$

As seen in Figure 11, K_t always increases with decreasing (r), but K_f passes through a maximum (K_{fmax}) at r_{crit} equal to "a" in Peterson's equation (Eq. 7). K_{fmax} should be the largest possible value of K_f for the weld shape and material in question. Because "a" is dependent upon the ultimate strength (S_u), higher strengths steels will have higher values of K_{fmax} for the same weld shape (Figure 12). In addition, K_{fmax} depends upon the shape of the weld and the loading to which it is subjected (α), and upon the size or scale of the weldment (t). These facts and Eq. 6 lead to two interesting results: the fatigue crack initiation life should depend upon ultimate tensile strength (S_u) and upon the size of the weldment (t).

Using Eq. 8 and the observed variation in fatigue properties with hardness (Figure 10), Eq. 6 can be rewritten:

$$S_a = \frac{S_u + 50 - \sigma_r}{1 + .053\alpha\ S_u t^{\frac{1}{2}}}\ [2N_I]^{-\frac{1}{6}\ \log 2\ (1 + \frac{50}{S_u})} \qquad (9)$$

where: S_a is the fatigue limit at $2N_I$ (R = -1), and σ_r is the residual stress at weld toe. The fatigue limit of steel weldments predicted by Eq. 9 is a function of S_u and is plotted in Figure 13 for three assumptions of weld toe residual stress (σ_r). For the assumption of no residual stress, it can be seen that the fatigue resistance of a steel weldment

continues to increase with increasing S_u even though the increase in σ_f' due to the increase in S_u is partially offset by a larger K_{fmax}. Under the assumption of positive residual stresses equal to the base metal yield strength ($\sigma_r = +S_y$), the fatigue limit is no longer a strong function of S_u but increases only slightly and then decreases with increases in S_u above 80 ksi. Thus, increasing the strength (S_u) of weldments (particularly in the as-welded condition) may actually decrease their fatigue limit due to the combined effects of increasing K_{fmax} and σ_r. The full potential of higher strength steels may be realized if the welds are stress relieved, that is, if the residual stresses (σ_r) are reduced from + S_y to 0. Furthermore, the higher strength steels should show the greatest benefit from over-stressing or inducing compressive residual stresses ($\sigma_r = -S_y$) at the weld toe.

The K_{fmax} concept also predicts a dependence of fatigue life upon the scale of the weldment (Eq. 8). If one considers <u>geometrically similar</u> welds having a cruciform shape (see Shape B, Figure 5) of various sizes, K_{fmax} should depend upon $(t)^{\frac{1}{2}}$ and should vary with the size of the weldment as shown in Table 2. Thus, when N_I is a major portion of life (not necessarily the case for mild steel weldments, Figure 14) the fatigue resistance of a weld should depend strongly upon its size. N_P should also depend upon scale but to a lesser degree.

PREDICTING THE FATIGUE CRACK PROPAGATION LIFE (N_p)

The fatigue crack propagation life (N_p) may be estimated through the observed dependence of the crack growth rate (da/dN) upon the range of stress intensity factor (ΔK). A simple representation of this dependence is the Paris Power Law (16):

$$\frac{da}{dN} = C\,(\Delta K)^n \tag{10}$$

where: $\frac{da}{dN}$ is the crack growth rate, ΔK is the range in stress intensity factor, and C,n are material, loading condition, and environmental constants. This expression can be integrated to obtain N_p:

$$N_p = \frac{1}{C}\int_{a_I}^{a_F} \Delta K^{-n}\, da \tag{11}$$

where: a_I is the initial crack size and a_F is the final crack size. The range in stress intensity factor (ΔK) is a function of the remote stress range (ΔS), the current value of crack length (a) and a geometry factor (Y):

$$\Delta K = Y\Delta S(\pi a)^{\frac{1}{2}} \tag{12}$$

There are few values of Y available for weld shapes (17-20). The geometry factor Y usually must be determined for each weld shape - often a difficult task. Maddox (19) has shown that Y may be considered to be the superposition of several effects:

$$Y = \frac{M_s\, M_t\, M_k}{\phi_o} \tag{13}$$

where: M_s is a magnification factor which corrects for the presence of a free surface (1.12), M_t is a magnification factor which corrects for finite plate width $(\sec \pi a/2w)^{\frac{1}{2}}$, M_k is a magnification factor which corrects for

the stress concentration of the weld discontinuity in question, and ϕ_o is a correction factor for crack shape. If one can assume that the propagating fatigue crack has a more or less constant shape or, as in the case of a weld toe, that it rapidly becomes a line-crack through the multiple initiation of fatigue cracks at the toe, then the biggest remaining problem for the application of Eq. 12 is determining the geometrical correction factor (M_k) which is usually a function of crack length (a).

Using a method for the determination of M_k based on the principle of elastic superposition (18) and Emery's solution (21) for a edge-crack subjected to an arbitrary system of crack opening stresses (Figure 15), one can determine the stress intensity factor for a complex shape such as a weld from the results of a single, finite-element analysis of the uncracked body (Figure 4):

$$\Delta K = (\pi a)^{\frac{1}{2}} \left[1.12\,\sigma_a - \int_o^a f(x/a)\,\frac{d\sigma}{dx}\,dx\right] \qquad (14)$$

$$f(x/a) = .8(x/a) + .04\,(x/a)^2 + 3.62\text{x}10^{-6} \exp 11.8\,(x/a)$$

Albrecht (22) has recently given an expression for f(x/a) which is similar to Emery's but simpler:

$$f(x/a) = 1.12\,\frac{2}{\pi}\,\sin^{-1}\,(x/a) \qquad (15)$$

The material properties (C,n) in Eq. 10 have been determined for the metallurgical zones found in welds (23-25). Factors influencing the fatigue crack growth rate such as stress ratio and environment affect welds in much the same manner as they do other notched metal members and will not be discussed here (12, 26, 27).

PREDICTING THE TOTAL FATIGUE LIFE (N_T)

The total fatigue life (N_T) is considered to be the sum of the crack initiation life and (N_p) the fatigue crack propagation life (Eq. 1). When initiation occurs at an obvious defect such as a pore, slag pocket or deep notch, the size of the initiated crack length (a_I) may be taken as the dimension of the defect. Thus, the fatigue crack propagation life (N_p) may be calculated directly from Eq. 11 taking the defect size as a_I and added to the estimate of N_I using Eq. 6 (naturally in the case of serious defects N_I may be rather short) to obtain N_T. Problems arise in the instance of weld discontinuities such as weld toes which are serious defects but not deep notches. In this case, the value of the initiated crack length (a_I) is not clear. It has been past practice to assume arbitrarily that a_I was .01-in. regardless of the stress level or the material (9). The British Welding Institute researchers have back-figured values of a_I for some materials which permit one to estimate N_T as though it were entirely devoted to fatigue crack propagation (10, 28).

Recent work by Chen (29) has provided an alternative strategy for the definition of a_I. For fatigue failure to occur, an a_I just greater than the length of a non-propagating crack (a_{th}) must be provided by the process of fatigue crack initiation. Thus, at long lives, a_I should be just a little larger than a_{th}. From Chen's (29) work it can also be argued that a_I is the distance from the notch root at which the stress diminishes to a value $K_f \Delta S$. Since from the K_{fmax} concept ($K_{fmax} - 1$) is one half of ($K_t - 1$), one can determine a_I for a shape such as a weld if the profile of stress inward from the fatigue initiating notch can be determined (as for the cruciform weld in Figure 4).

Using the approximation to the finite element analyses results shown:

$$\sigma_{xx}/S - 1 = (K_t - 1) \exp(-35 (K_t - 1) (x/t)) \quad (16)$$

One can rewrite Eq. 16 defining $(\sigma_{xx}/S - 1)$ at a_I as being $(K_{fmax} - 1)$. Since for the K_{fmax} condition q must be 1/2 and since r must be equal to "a":

$$q = \frac{K_{fmax} - 1}{K_t - 1} = \exp(-35 \alpha (t/a)^{\frac{1}{2}} a_I/t) = 1/2 \quad (17)$$

Solving Eq. 17 for a_I:

$$a_I = .1878\, t^{\frac{1}{2}}/(\alpha S_u) \text{ (for steels)} \quad (18)$$

From Eq. 18, a_I should depend upon the weld geometry (α), the scale of the weldment $(t)^{\frac{1}{2}}$, and the strength of the material (S_u). For a mild steel butt weld (t = 1.0 in., α = .23, S_u (HAZ) = 90 ksi), Eq. 18 predicts an a_I of .01 in.

ESTIMATING THE INFLUENCE OF WELD RESIDUAL STRESSES ON N_I

If the mean stress relaxes during cycling, the current value of mean stress (σ_o) may be estimated by (30):

$$\sigma_o / \sigma_{os} = (2N_i - 1)^k \tag{19}$$

where: σ_o is the current value of mean stress (notch root), σ_{os} is the initial value of mean stress (notch root), $2N_i$ is the elapsed reversals, and k is the relaxation exponent (a function of strain amplitude). Assuming that the notch root strains are essentially elastic ($2N_I > 2N_{tr}$), the damage per cycle is:

$$(1/2N_I) = \left[(\sigma_f' / \sigma_a)(1 - \sigma_o / \sigma_f')\right]^{-1/b} \tag{20}$$

Using the Palmgren-Miner rule of cumulative damage and Eqs. 19 and 20, the fatigue crack initiation life under conditions of relaxing mean stress can be calculated by integrating the Eq. 21 (below) and solving for the upper limit of integration using approximate methods (31).

$$\int_1^{2N_I} \left[(\sigma_f'/\sigma_a)(1 - \sigma_{os}\,(2N_i)^k/\sigma_f')\right]^{-1/b} dN = 1 \tag{21}$$

Equation 21 affords a means of predicting the potential effects of weld toe residual stresses (σ_r) on the fatigue crack initiation life, N_I. It is assumed that σ_r approaches the yield point of the base metal (S_y) in the small volume at the weld toe in which initiation takes place. This residual stress and any remotely imposed mean stress may relax with cycling (Eq. 19). The notch root residual stresses have been ignored in the calculation of N_p, but the remote mean stress effects are considered to persist and to influence the propagation portion of life through the reported variation of crack opening factor as a function of stress ratio (R) (32).

The residual stress (σ_r) is assumed to be either $+S_y$, 0, or $-S_y$. These three cases cover most possibilities. The worst case ($\sigma_r = S_y$) is often approached in practice. The intermediate case ($\sigma_r = 0$) would result from stress relief. The most favorable case ($\sigma_r = -S_y$) could be realized through some mechanical pretreatment such as shot-peening or over-stressing.

The initial value of notch root mean stress (σ_{os}) resulting from the residual stress (σ_r) and remote mean stress (e.g., R = 0) may vary greatly depending upon the material (Figures 16 and 17). For many aluminum alloys the HAZ at the weld toe is in the zero-temper state; consequently, the notch-root plasticity in the first cycle results in $\sigma_{os} = 0$. Other materials, such as high strength steels, may exhibit very little notch-root plasticity; consequently, σ_{os} may be larger than σ_r. The results obtained using the model agree with the experimentally observed behavior (31).

The predictions for the high-strength, quenched-and-tempered steels (Figure 18) indicate that such materials can sustain high residual stresses which do not relax. The total fatigue life of such materials should be strongly influened by both residual stress (σ_r) and stress ratio (R). Stress relief or mechanically induced compressive residuals should be highly effective.

Mild steels (Figure 19) may have large stabilized mean stress (σ_{os}) but, since the transition fatigue life (N_{tr}) is often very long ($\approx$ 500,000 cycles), there is considerable notch-root plasticity even at long lives (10^6 cycles). This notch-root plasticity tends to relax rapidly the notch-root mean stresses with the result that N_I and N_T

are little affected for N_T less than 10^6 cycles (Figure 19). The observed dependence of N_p on stress ratio does, however, result in the prediction of a variation in N_T with stress ratio (R).

Because of the high notch-root plasticity during the first few cycles (before the material cyclically hardens), the aluminum weld considered here (5083/5183) exhibits little dependence upon either (post fabrication) residual stress or stress ratio, even though the relaxation of the stabilized mean stress (σ_{os}) is very slow (Figure 20).

Generally, the mean stress relaxation exponent (k) in Eq. 19 decreases with the transition fatigue life (N_{tr}). Other things being equal, materials with short N_{tr} do not exhibit rapid relaxation of mean stresses; and N_I in such materials should be influenced by σ_r and R. (The aluminum considered is an exception to this rule for the reasons discussed.)

PREDICTING THE TOTAL FATIGUE LIFE OF WELDS CONTAINING INTERNAL DEFECTS

Although the fatigue crack initiation life of welds containing internal defects (porosity, slag, incomplete joint penetration, etc.) could be predicted using existing models for K_t, it often develops (as in the case of incomplete joint penetration) that the notch-root cannot be described by a single radius. Most internal weld defects are sufficiently irregular that one is forced to assume that any value of notch-tip radius may occur somewhere. Thus, even for the smoothest and most regular of internal defects it is not possible always to characterize their notch-root radius by a single value. A solution to this difficulty is the use of the K_{fmax} concept (10).

One can represent most internal defects as elliptical flaws having as their largest dimension the semi-major axis of the ellipse (c) and having an unknown and variable notch-root radius (r):

$$K_t - 1 = \alpha \, (c/r)^{\frac{1}{2}} \tag{22}$$

where: α is the coefficient for the defect for the loading condition ($\alpha = 2$, infinite body, axial loading, see also Table 1). From Eq. 7 and Eq. 22, $K_{fmax} - 1$ would be:

$$K_{fmax} - 1 = (\alpha/2)(c/a)^{\frac{1}{2}} \simeq .053\alpha \, S_u c^{\frac{1}{2}} \text{ (for steel)} \tag{23}$$

It can be seen from Eq. 23 that K_{fmax} (which largely controls N_I) depends upon the size of the defect (c) and the ultimate strength of the material (S_u) but does not depend upon the size of the weldment (t) in which it is found unless the defect interacts with the surface or other weld discontinuities. The N_I of a weld containing an elliptical defect can be estimated using Eq. 23 and Eq. 6. The N_p of a weld containing a defect

can be estimated using Eq. 11 and the "appropriate" (often the largest) defect dimension as a_I. There is one important exception to this generalization: the most critical dimension of an elongated defect in a weld is not its length along the axis of the weld but its through-thickness dimension (which usually cannot be measured on a normal incidence radiograph). Other difficult problems can usually be solved by finding the appropriate fracture mechanics model (22) or by recourse to the use of Eqs. 14, 15.

As an example of the entire method for predicting the fatigue resistance of weldments and of the typical results using it, two nearly identical cruciform weldments (Figure 5B, Table 3) were tested to failure and the total fatigue life was estimated from hardness readings, Eqs. 1, 11, 21 and Figure 10. The two weldments (A, B) were identical and contained LOP ($2c/t = .62$) except that A was subjected to 0 - 30 ksi and B was subjected to 0 - 22 ksi. Another very important difference was that A had an appreciable joint distortion (ζ) such that a bending stress (ΔS_B = 21 ksi.) was generated at peak load; whereas, B had no bending stress ($\Delta S_B = 0$). Because of the insensitivity of the LOP defect to bending stresses (Table 1), the presence or absence of bending greatly influences the fatigue life and the location of failure (Table 3).

Thus, a rational approach to rating the severity of an internal defect in fatigue applications would be to compare the expected N_T due to fatigue failure at the defect with the expected N_T due to weld discontinuities necessarily present (weld toes). A defect causing failure before the weld toe must be considered as detrimental; whereas, one which could not cause failure would be innocuous. From the K_{fmax}

concept and the model reviewed here, it is clear that the relative severity of an internal defect will depend upon the scale of the weldment (t), upon the absolute size of the defect (c), upon material properties (S_u), upon the shape of the weldment (α^{toe}, α^{defect}), and upon the type of loading (internal defects near the neutral axis of a weldment subjected to bending may not be seriously stressed). For example for axial loading, the radio (K^{LOP}_{fmax} - 1) for the LOP in the cruciform weld (Figure 5B) to that of the weld toe (K^{TOE}_{fmax} - 1) may be written as:

$$(K^{LOP}_{fmax} - 1) \; / \; (K^{TOE}_{fmax} - 1) = (\alpha^{LOP}_{A} \; S^{LOP}_{u} \; / \; \alpha^{TOE}_{A} \; S^{TOE}_{u}) \; (c/t)^{\frac{1}{2}} \qquad (24)$$

Thus for axial loading, an LOP defect in a cruciform weldment should become more serious a fatigue initiation site (at long lives $N_T \simeq N_I$) than the weld toe when the value of Eq. 24 exceeds 1.

ACKNOWLEDGEMENTS

The studies which this review summarizes were principally supported by the University of Illinois Fracture Control Program which is funded by a consortium of midwest industries.

The authors wish to thank Professor JoDean Morrow of the Department of Theoretical and Applied Mechanics for his advice and help over the years. Special thanks are extended to Professor William H. Munse of the Department of Civil Engineering, for many stimulating discussions which helped give direction to the studies summarized here and for many helpful comments made during the writing of this review.

REFERENCES

1. Munse, W.H. 1964. Fatigue of Welded Structures, New York, NY: Welding Research Council. 210 pp.

2. Gurney, T.R. 1979. Fatigue of Welded Structures, Cambridge: Cambridge University Press. 410 pp.

3. Sanders, W.W. 1972. Welding Research Council Bulletin No. 171. 30 pp.

4. Mann, J.Y. 1970. Bibliography on the Fatigue of Materials, Components and Structures, Vols. I and II, Oxford: Pergamon, 316 pp. 489 pp.

5. Stephens, B.A., Zoro, R.C. 1970. Bibliography on the Fatigue of Welded Structures, Abbington: The British Welding Institute, 121 pp.

6. Reemsnyder, H.S. 1978. Bibliography on the Fatigue of Weldments. Welding Journal. 57: 178s - 182s.

7. Radziminski, J.B., Srinivasan, R., Moore, D., Thrasher, C. and Munse, W.H. 1973. Structural Research Series No. 405, University of Illinois at U-C., Urbana, Illinois

8. Sanders, W.W., Jr and Lawrence, F.V., Jr., 1978. ASTM STP 648, pp. 22-34.

9. Lawrence, F.V., Jr., Mattos, R.J., Higashida, Y., and Burk, J.D. 1978. ASTM STP 648, pp. 134-158.

10. Tobe, Y. and Lawrence, F.V. Jr., 1976. The Effect of Inadequate Joint Penetration on the Fatigue Resistance of High-Strength Structural Steel Welds. Welding Journal. 56:9: 259s - 266s.

11. Mattos, R.J. and Lawrence, F.V., 1977. SP - 424, Society of Automotive Engineers, Warrendale, Pa.

12. Burk, J.B. and Lawrence, F.V., 1977. Influence of Bending Stresses on the Fatigue Crack Propagation Life in Butt Welds. Welding Journal 56:2: 56:2: 615s - 665s.

13. Higashida, Y., Burk, J.D. and Lawrence, F.V., Jr., 1978. Strain-Controlled Fatigue Behavior of ASTM A36 and A514 Grade F Steels and 5083-O Aluminum Weld Materials. Welding Journal 57:334s - 344s.

14. Basquin, O.H. 1910. The Exponential Law of Endurance Tests. Proc. ASTM 10:625

15. Peterson, R.E. 1974. Stress Concentration Factors, New York: John Wiley. 317 pp.

16. Paris, P.C. and Erdogan, F. 1963. A Critical Analysis of Crack Propagation Laws. Trans. ASME, J. Basic Eng. 85: 528

17. Tarada, H. 1976. An Analysis of the Stress Intensity Factor of a Crack Perpendicular to the Welding Bead. Eng. Fract. Mech. 8:441-444.

18. Lawrence, F.V., Jr. 1973. Estimation of Fatigue Crack Propagation Life in Butt Welds. Welding Journal 52: 212s - 220s.

19. Maddox, S.J. 1974. Assessing the Significance of Flaws in Welds Subject to Fatigue. Welding Journal 53: 401s - 409s.

20. Frank, K.H. 1971. Lab Report No. 358.37 Fritz Engineering Laboratory, Lehigh University, Bethlehem, Pa.

21. Emery, A.F. 1966. Stress-Intensity Factors for Thermal Stresses in Thick Hollow Cylinders. J. Basic Eng., ASME Trans Series D. 88:45.

22. Albrecht, P. and Yamada, K. 1977. Rapid Calculation of Stress Intensity Factors. J. Str. Div of ASCE 2:377 - 389

23. Maddox, S.J. 1970. Fatigue Crack Propagation in Weld Metal and HAZ. Met. Const. and Brit. Weld Jrnl. 2:258 - 289.

24. Griffiths, J.R., Mogford, J.L., and Richards, C.E. 1971. Influence of Mean Stress on Fatigue Crack Propagation in a Ferritic Weld Metal. Metal Science Journal 5:150-154

25. Parry, M., Nordberg, H. and Hertzberg, R.W. 1972. Fatigue Crack Propagation in A514 Base Plate and Welded Joints. Welding Journal 51:485s - 490s.

26. Forman, R.G., Kearney, V.E., Engle, R.M. 1967. Numerical Analysis of Crack Propagation in Cyclic-Loaded Structures. Trans. ASME, J. Basic Eng. 89:459

27. Kapadia, B.M. 1978, ASTM STP 648, pp. 244-260.

28. Gurney, T.R. 1976. Finite Element Analyses of Some Joints with the Welds Transverse to the Direction of Stress. Weld Res. Abd. 22:2 - 29.

29. Chen, W.C., and Lawrence, F.V. 1979. Fracture Control Program Report No. 32, University of Illinois at C-U, Urbana, Illinois

30. Jhansale, H. R. and Topper, T. H. 1973. ASTM STP 519 p. 246.

31. Burk, J.D. and Lawrence, F.V., Fracture Control Program Report No. 29, University of Illinois at Champaign-Urbana, Urbana, Illinois.

32. Elber, W. 1971. ASTM STP 486, p. 230.

33. Tucker, L.E., Landgraf, R.W. and Brose, W.R. 1974. Paper 740279 S.A.E. Automotive Engineering Congress.

Table 1 Elastic Concentration Coefficients[a] for Various Weldments

	Description	Geometry	α_A	α_B
A.	T-Joint, Full Penetration Welds (fixed ends)	$\Theta = 45^o$	0.35	0.19
B.	T-Joint, Fillet Welds[b] (cruciform)	$\Theta = 45^o$ $2c/t = 0$	0.35	0.19
		$\Theta = 45^o$ $2c/t = .5$	0.38	0.19
		$\Theta = 45^o$ $2c/t = .75$	0.41	0.19
		$\Theta = 45^o$ $2c/t = 1$	0.45	0.19
C.	Double Lap Joint Transverse Fillet Welds	$\Theta = 45^o$ $\ell/t = 1.0$	0.44	0.19
		$\Theta = 90^o$ $\ell/t = 1.0$	0.60	0.24
		$\Theta = 90^o$ $\ell/t = 0.5$	0.95	0.30
D.	Butt Joint Full Penetration Double-V Groove Welds	$\Theta = 10^o$ $\phi = 90^o$	0.013	-
		$\Theta = 15^o$ $\phi = 90^o$	0.18	-
		$\Theta = 30^o$ $\phi = 90^o$	0.23	-
		$\Theta = 45^o$ $\phi = 90^o$	0.27	0.165
E.	Single Lap Joint Double Transverse Fillet Welds	$\Theta = 45^o$ $x/t = 4$	0.47	-
		$\Theta = 45^o$ $x/t = 12$	0.35	-

[a] $K_t - 1 = \alpha\,(t/r)^{1/2}$; α_A = axial coefficient, α_B = bending coefficient

[b] K_t at LOP for axial loads $K_{tA}^{LOP} = 1 + 1.15\,(c/r)^{1/2}$

K_t at LOP for bending loads $K_{tB}^{LOP} = .0165\,(c/r)^{1/2}\,K_{tA}^{LOP}$

Table 2 Influence of Strength and Size on K_{fmax}[a] for Cruciform Weldment (α = .35)

Plate Thickness (in.)	K_{fmax} ASTM A36[b]	K_{fmax} ASTM A514[c]
1/4	1.92	2.96
1	2.84	4.91
2	3.60	6.53

a $K_{fmax} = 1 + .053\ \alpha\ S_u t^{\frac{1}{2}}$;

b S_u (A36 - HAZ) = 90 ksi

c S_u (A514 - HAZ) = 200 ksi

Table 3. Estimation of Fatigue Resistance for Two Cruciform Welds with LOP[a]

Quantity	Cruciform Weld A		Cruciform Weld B	
	TOE	LOP	TOE	LOP
ΔS_A (ksi)	30		22	
ΔS_B (ksi)	21		0	
t (in.)	.5		.5	
2c/t	.62		.62	
a(in.)	.008	.01	.008	.01
K^A_{fmax}(axial)	2.57	3.26	2.57	3.26
K^B_{fmax}(bending)	1.76	.68	1.76	.68
$\Delta\sigma\Delta\varepsilon$[b] (ksi.)	.44	.42	.11	.17
N_I(Eq. 21) (cycles)	1.36×10^5	2.20×10^5	1.47×10^7	4.28×10^5
N_p(Eq. 11) (cycles)	3.43×10^4	4.74×10^4	9.50×10^4	1.32×10^5
N_T(Eq. 1) (cycles)	1.70×10^5	2.67×10^5	1.48×10^7	5.70×10^5
N_T observed (cycles)	1.48×10^5	-	-	9.27×10^5

[a] See Figure 5 B

[b] $\Delta\sigma\Delta\varepsilon = (\Delta S_A K^A_{fmax} + \Delta S_B K^B_{fmax})^2 / E$

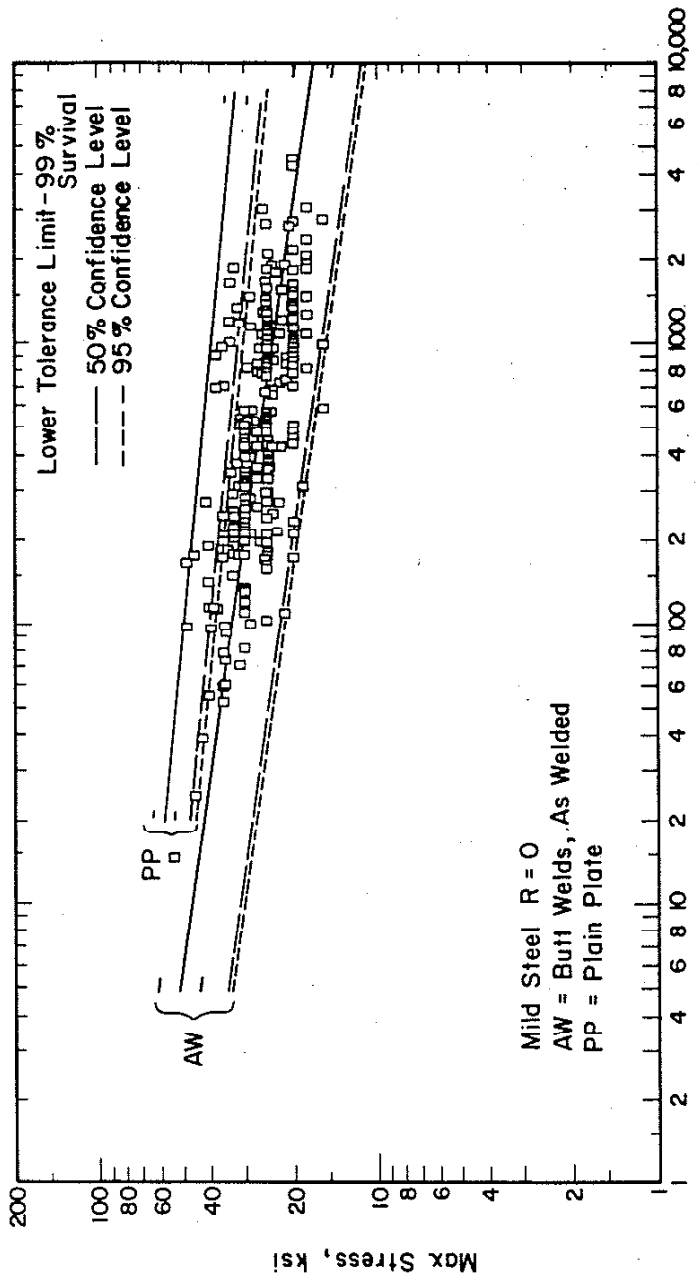

Figure 1. Stress range versus cycles to failure for mild steel butt welds subjected to zero to tension loading. The fatigue resistance of as-welded butt welds is generally less than the fatigue resistance of plain plate which is also indicated in the figure (7).

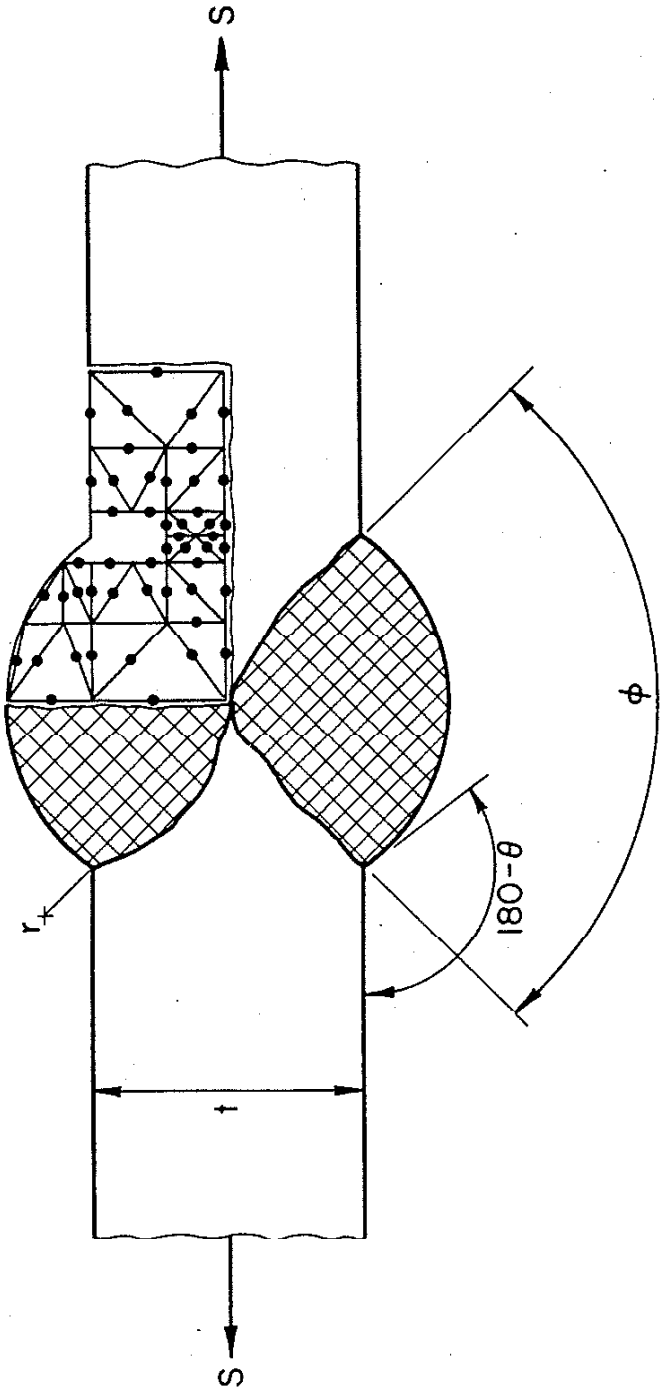

Figure 2. Parameters describing the shape of a double-V butt weldment. Inserted mesh shows the approximation of one quadrant of the weld by finite elements.

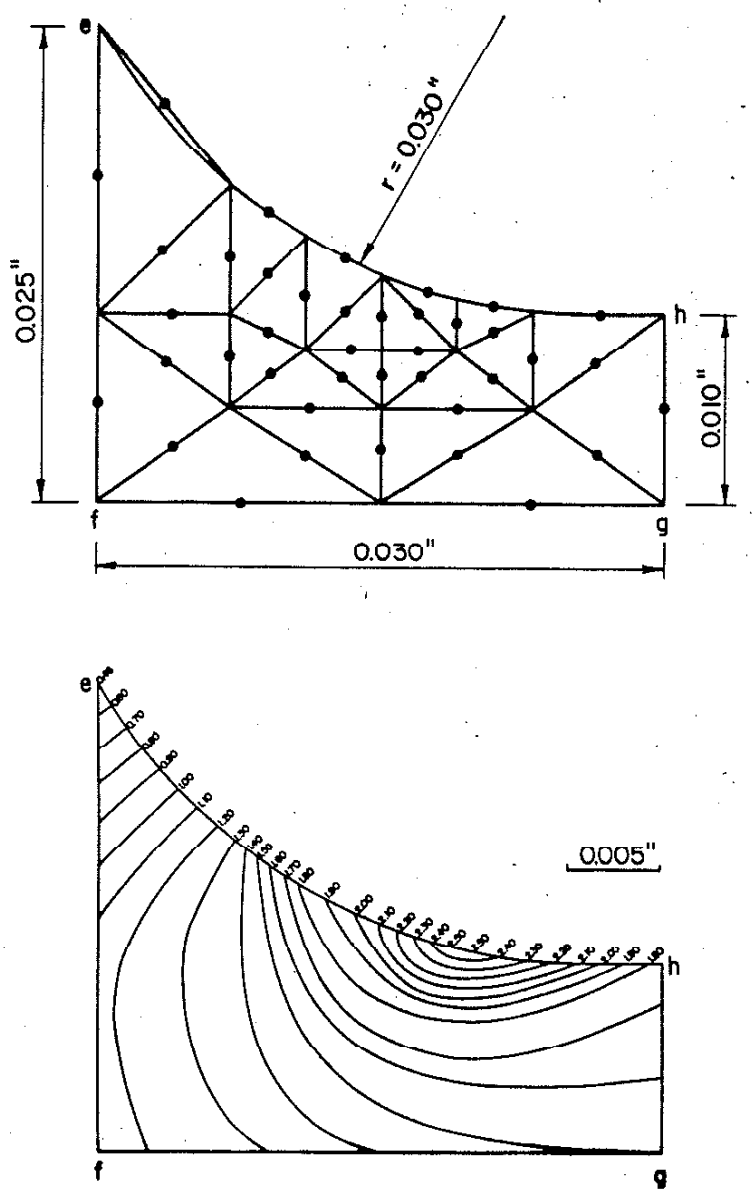

Figure 3. Finite element mesh representation of weld toe of weld in Figure 2 (above) and (below) the contours of the ratio of local stress to nominal stress (σ/S). Maximum stress is achieved in a very small region at the weld toe.

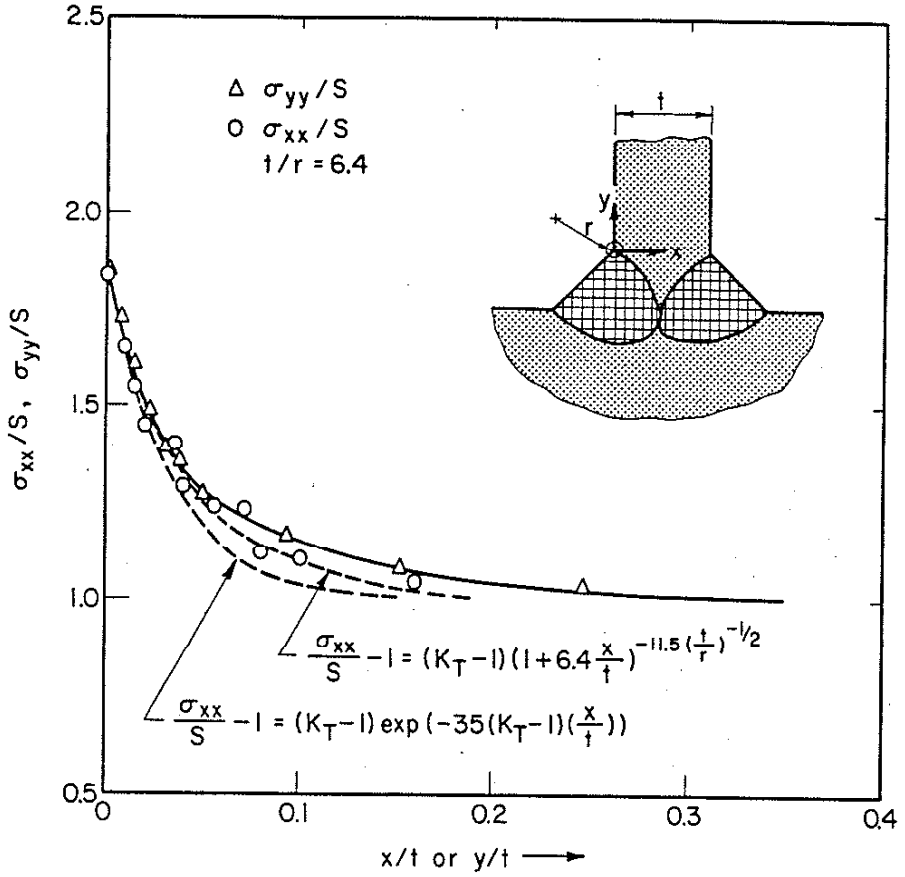

Figure 4. Variation of stress with distance away from the weld toe (σ_{yy}/S) and distance inward along the path the fatigue crack will follow (σ_{xx}/S). Two mathematical approximations to the finite element stress analysis results are indicated.

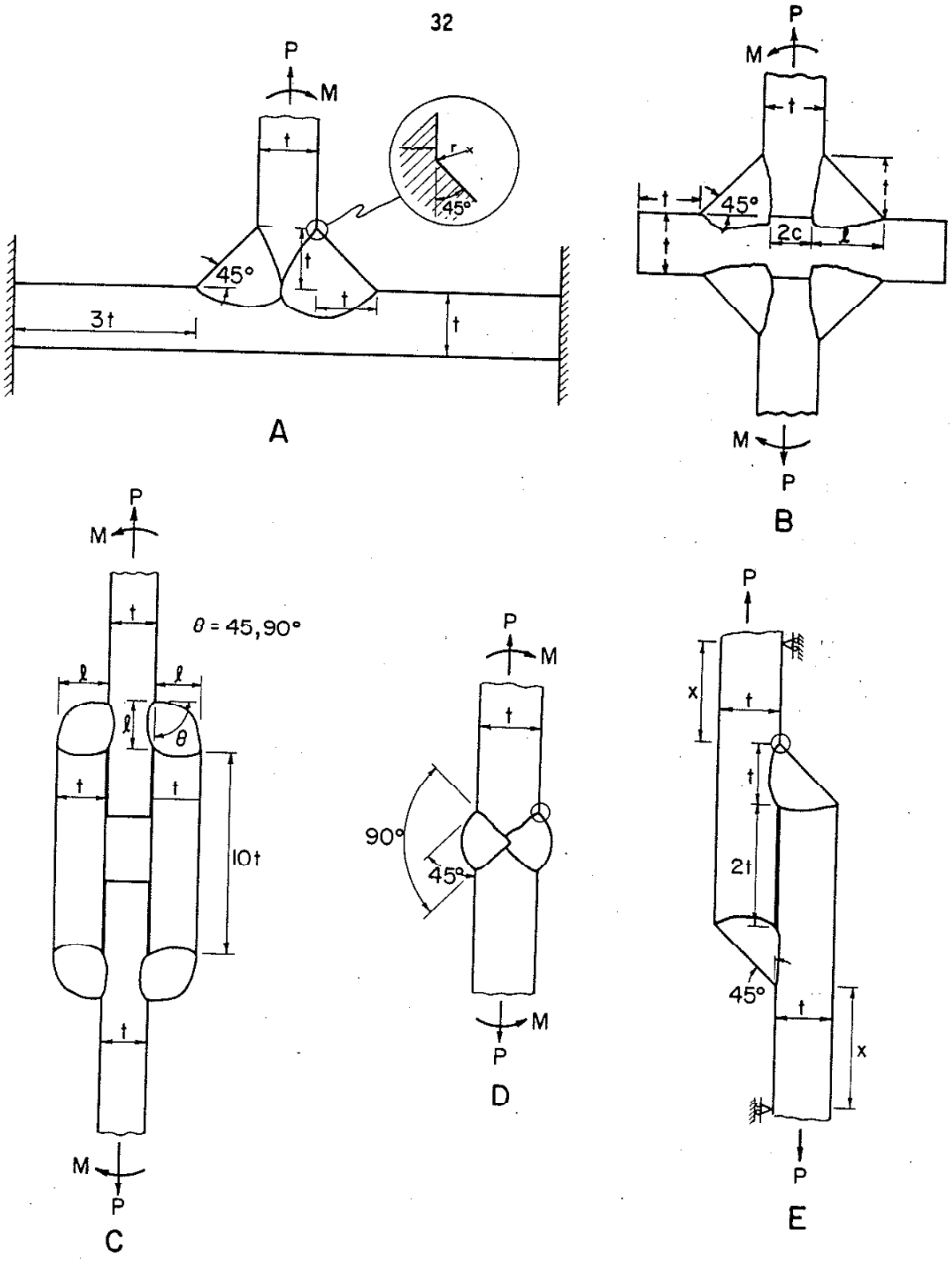

Figure 5. Geometry of the five welds analyzed.

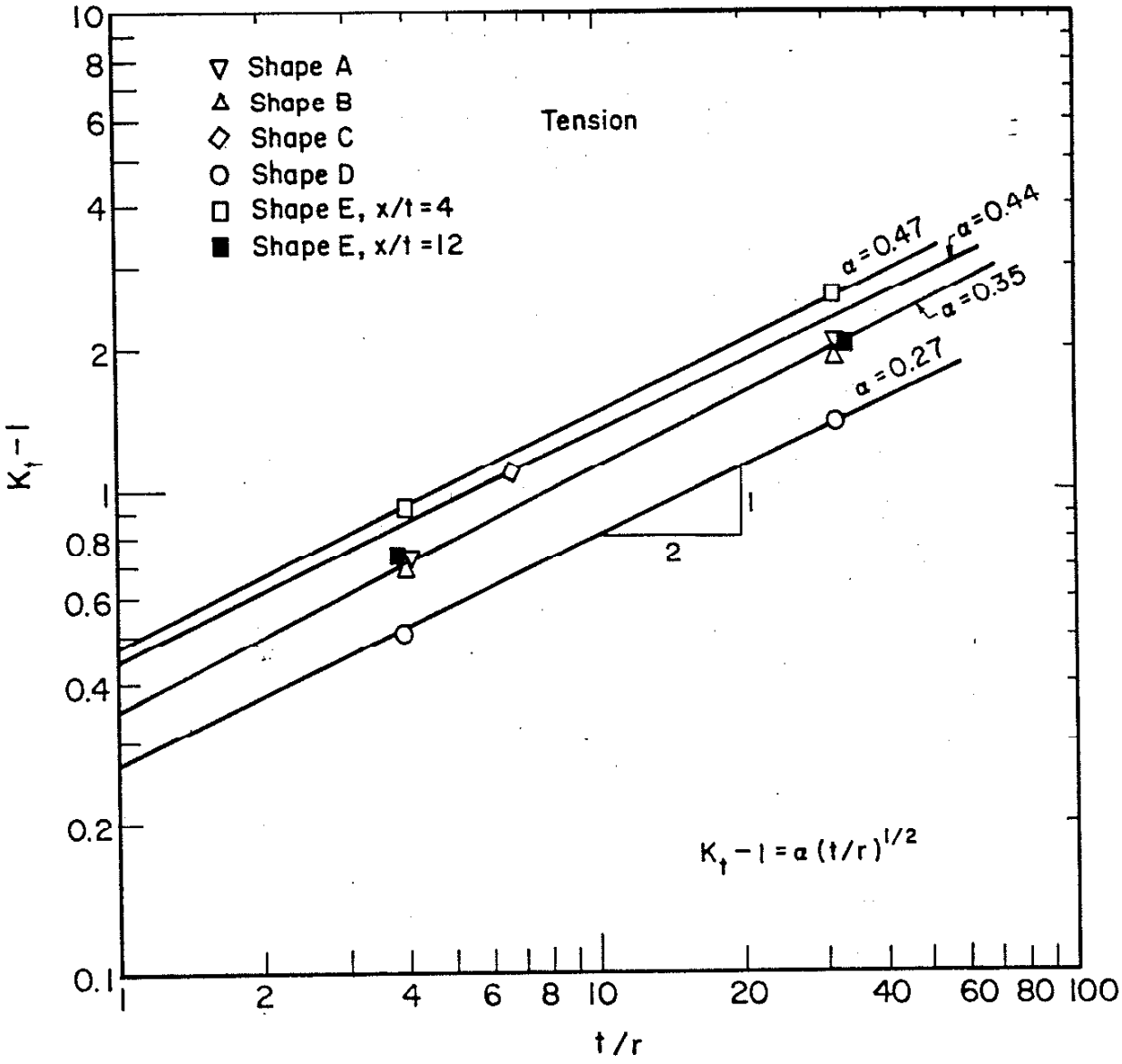

Figure 6. Variation of K_t - 1 with t/r for the five welds of Figure 5.

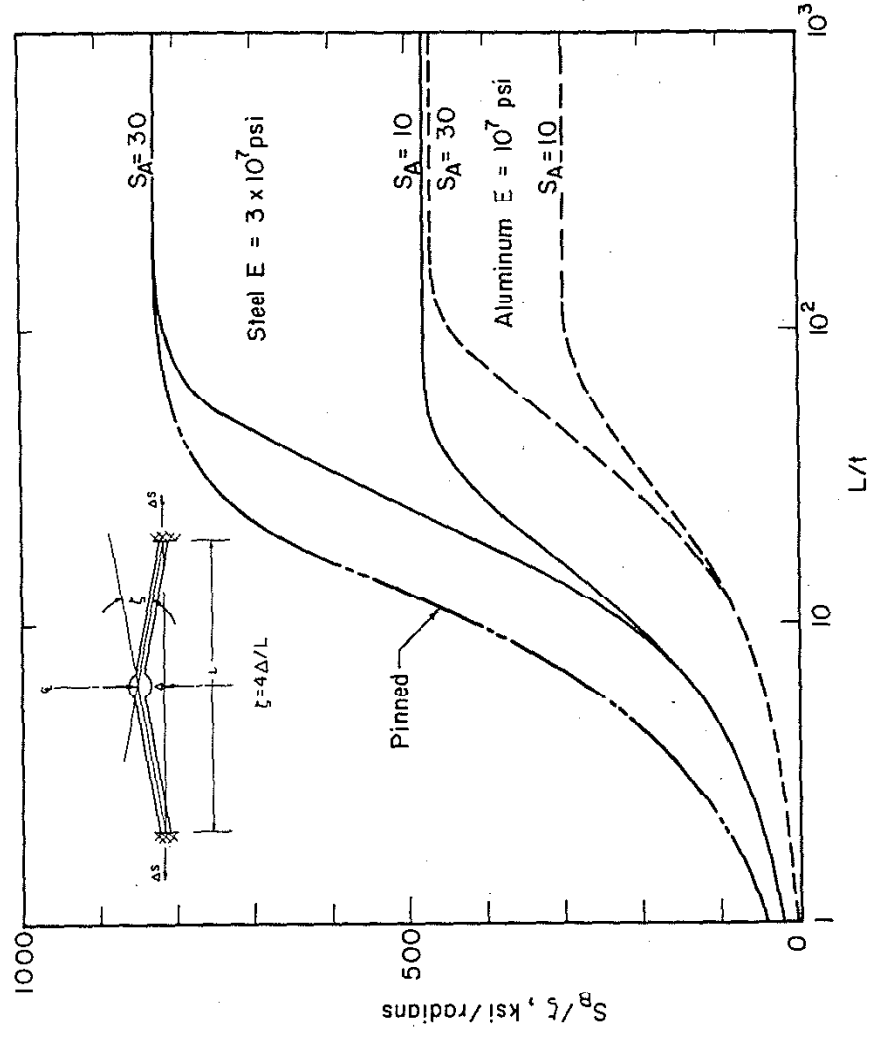

Figure 7. Ratio of bending stress to joint distortion ($\Delta S_B/\zeta$) as a function of the ratio of the length of weldment to its thickness (L/t). Unless otherwise indicated the results are for the fixed-end condition.

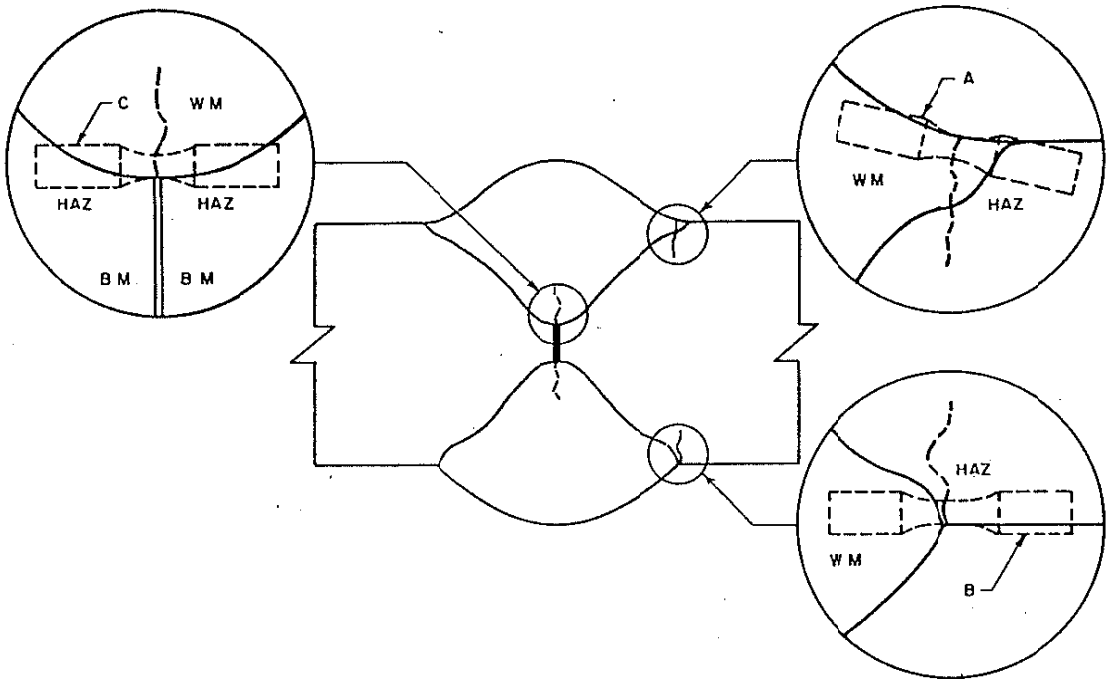

Figure 8. Typical locations of fatigue crack initiation in a butt weld. Fatigue cracks can initiate: in diluted, untempered weld metal (A); in the heat-affected-zone close to the line of fusion (B); and in tempered weld metal (C). The dashed-in fatigue specimens are laboratory smooth specimens which, if subjected to the local strains, should initiate a fatigue crack at the same life as the region in question (13).

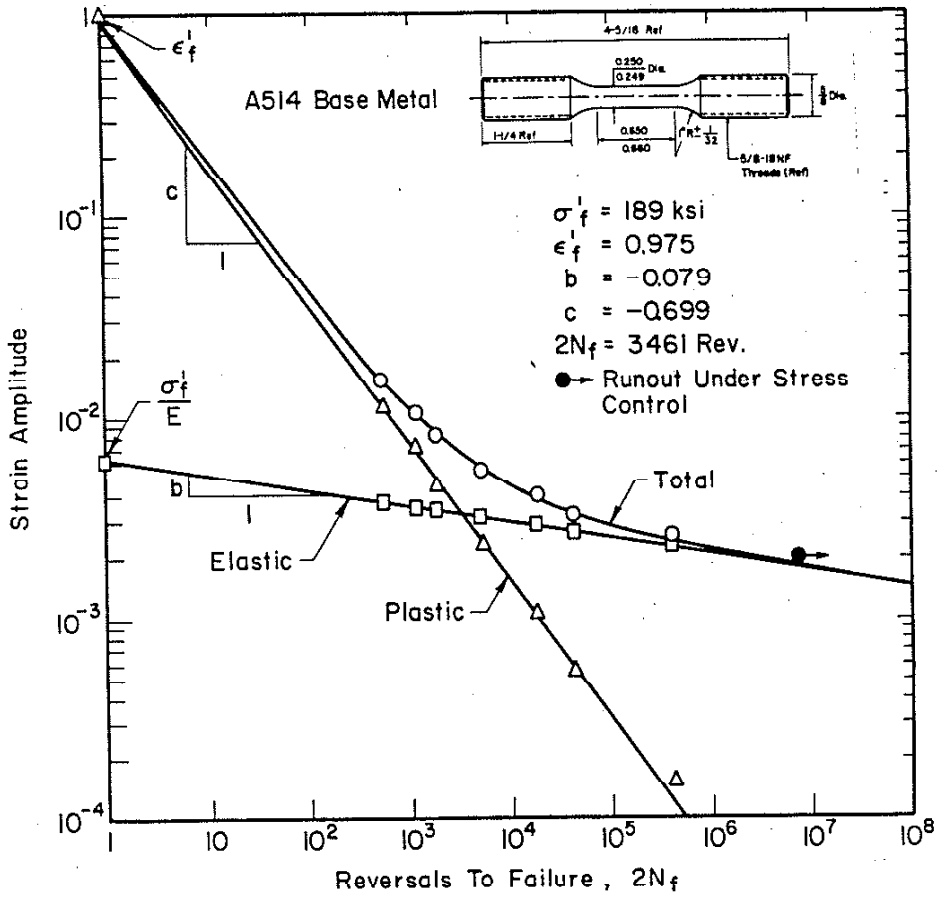

Figure 9. Strain-life data for ASTM A514 base metal. A typical smooth specimen for the determination of this data is insert. The strain-controlled fatigue properties ϵ'_f, σ'_f/E, b and c are indicated (13).

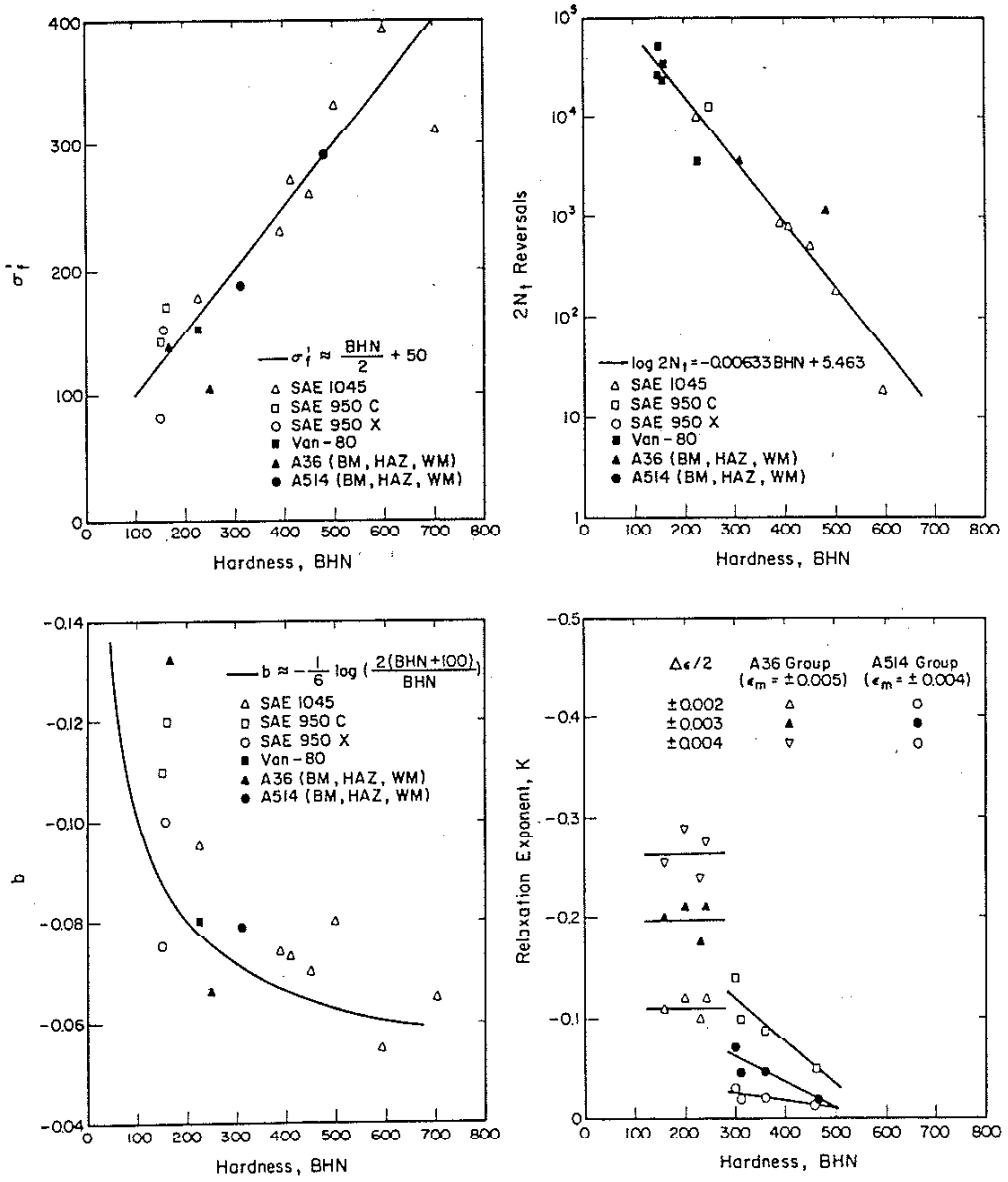

Figure 10. Variation of σ_f', b, $2N_t$, and k with Brinnel hardness (BHN) (13).

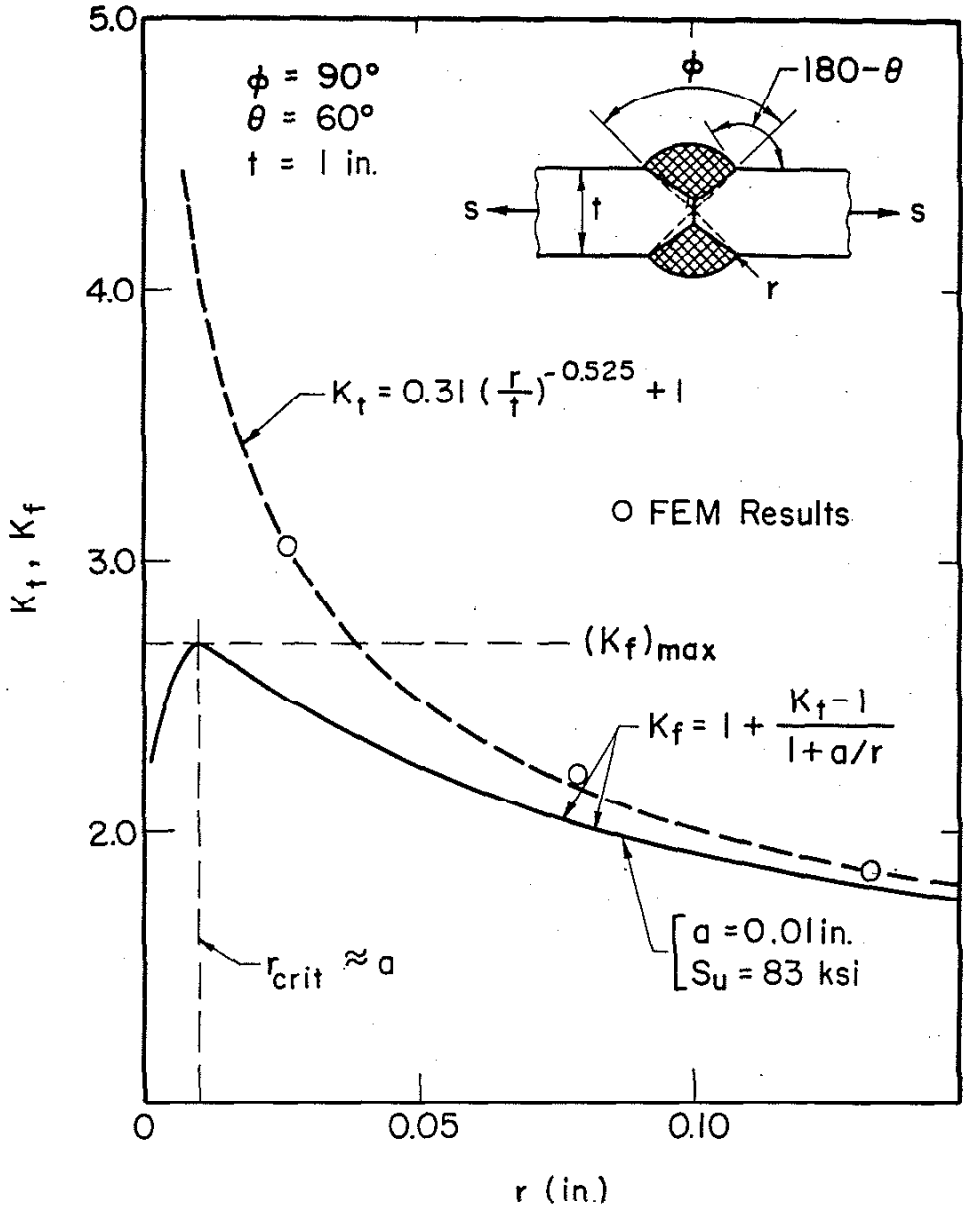

Figure 11. Elastic stress concentration factor (K_t) and fatigue notch factor (K_f) as a function of toe root radius. Open circles are the results of finite element stress analyses. The maximum value of fatigue notch factor (K_{fmax}) is indicated.

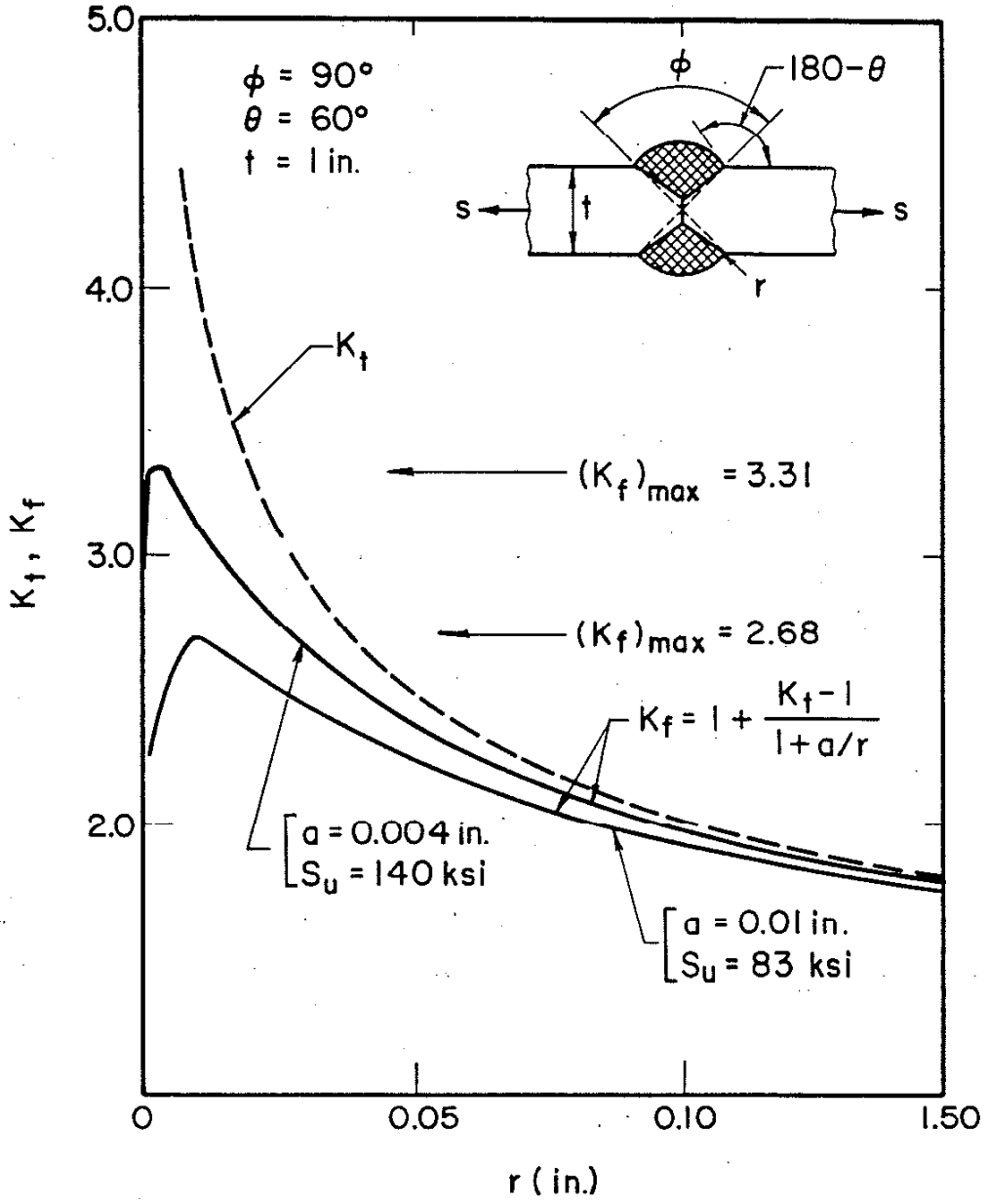

Figure 12. Variation of K_{fmax} with strength level (S_u) and consequent changes in the material parameter a.

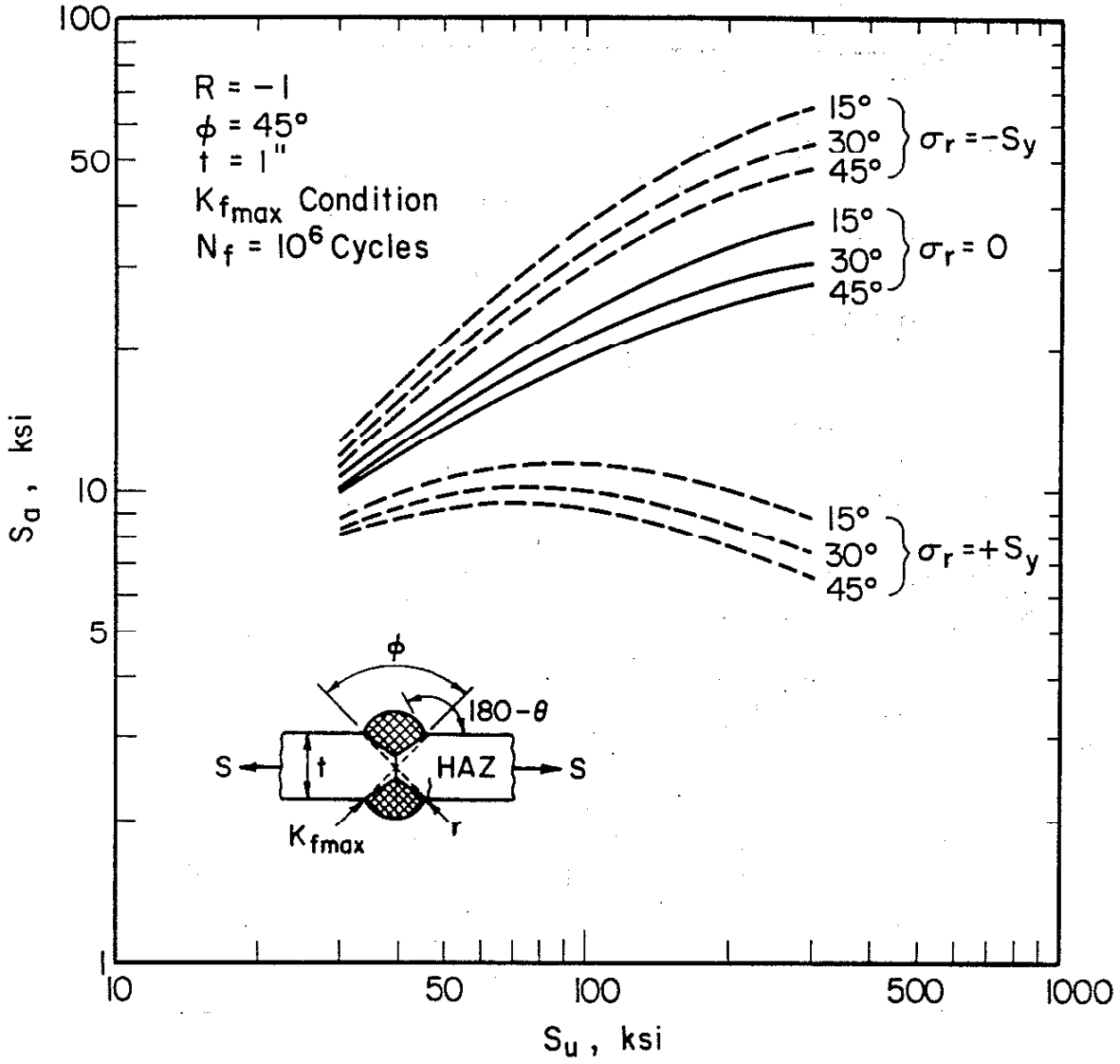

Figure 13. Predicted influence of ultimate strength (S_u) on the fatigue strength of a steel butt weldment at 10^6 cycles. The effect of weld shape (θ) and weld toe residual stresses (σ_r) are considered for assumed K_{fmax} conditions.

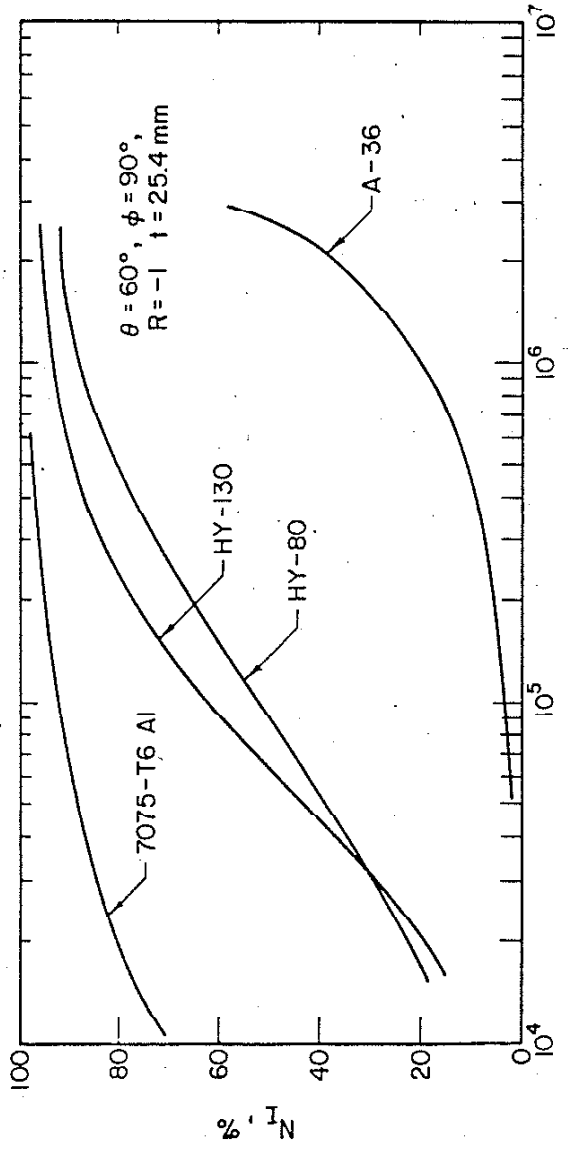

Figure 14. Predicted variation of percent of life devoted to crack initiation (N_I%) versus total life (N_T). K_{fmax} conditions and an initiated crack size of .01-in. are assumed for all materials.

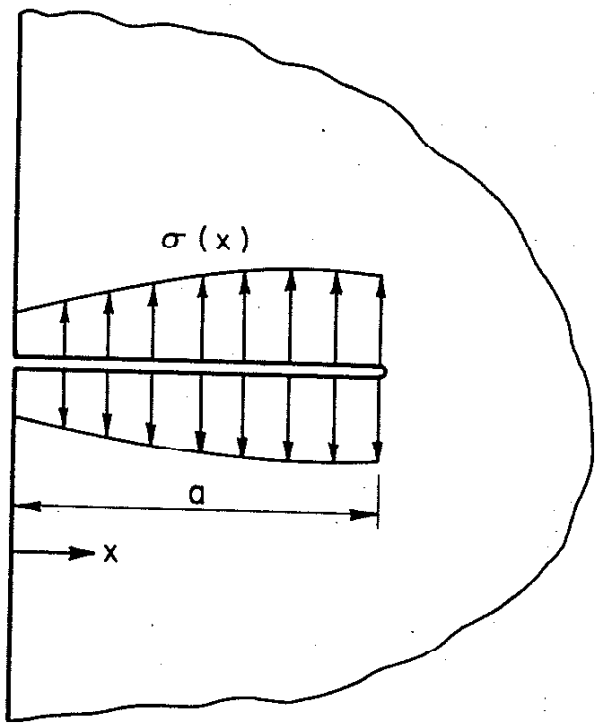

Figure 15. Edge crack loaded with an arbitrary system of surface stresses σ(x).

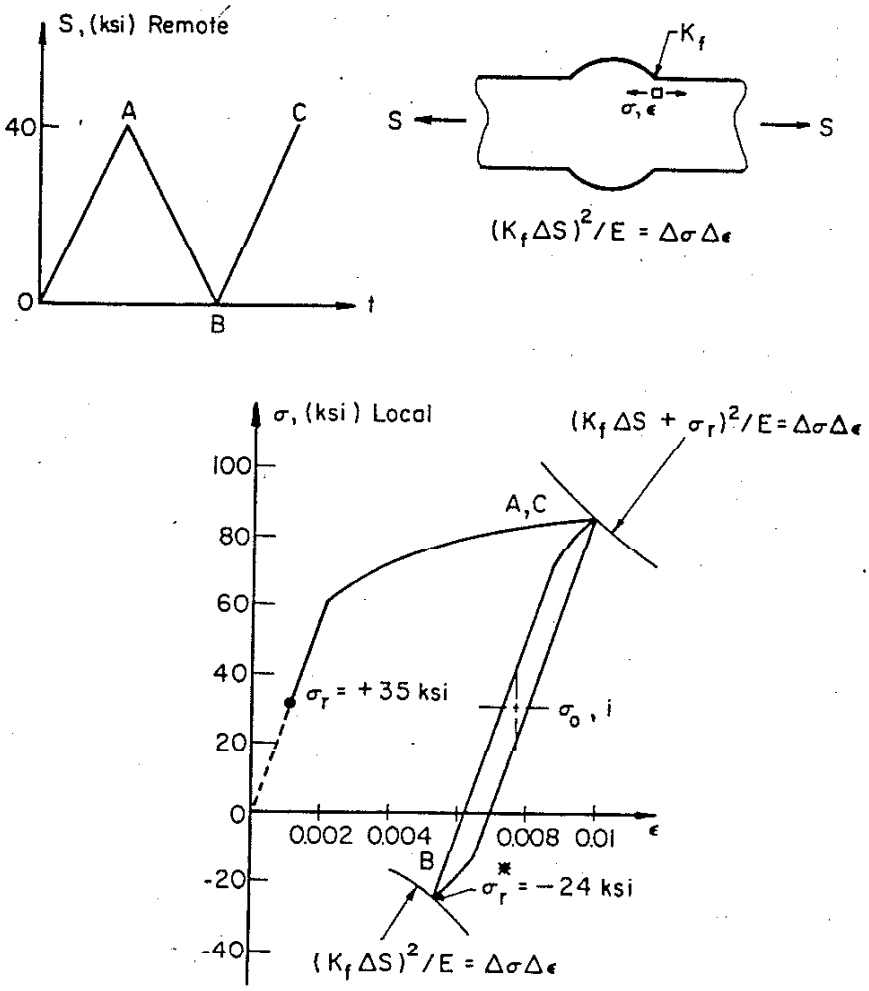

Figure 16. Simulated local stress-strain response at the weld toe for a butt weldment with weld-toe residual stresses (σ_r). (A36-HAZ material, σ_r = + 35 ksi).

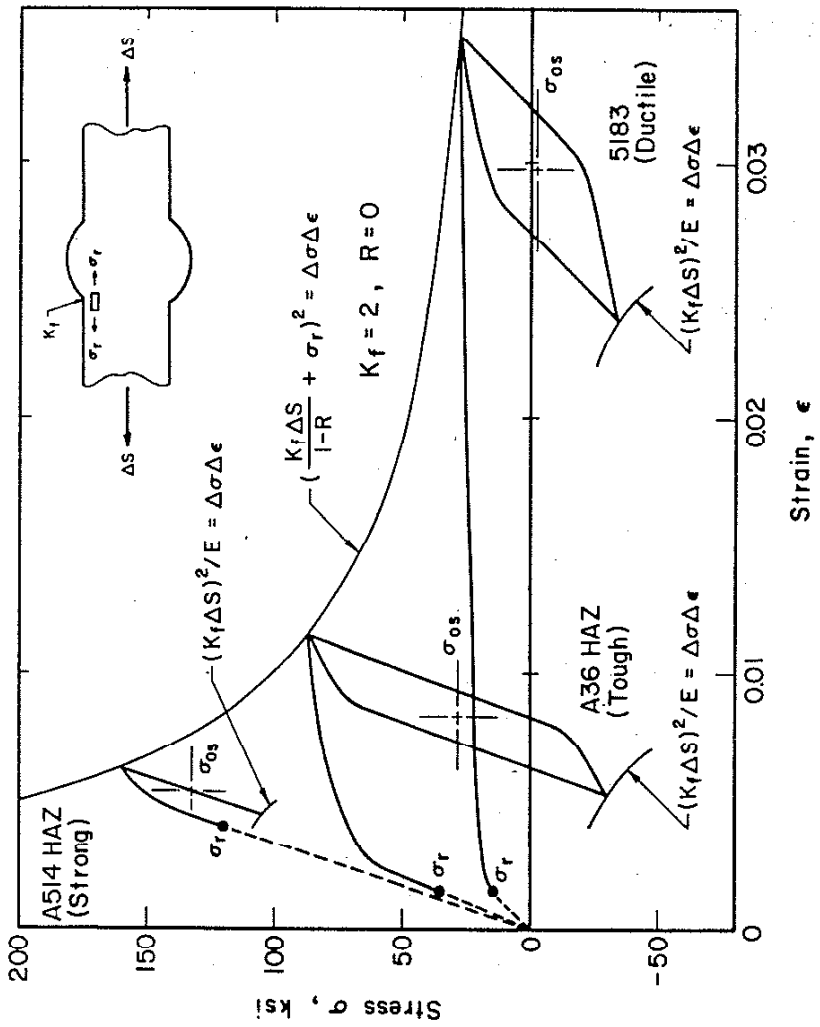

Figure 17. The initial value of mean stress (σ_{os}) resulting from three different extremes of material behavior. Results shown are for a single arbitrary value of $\Delta\sigma\Delta\epsilon$.

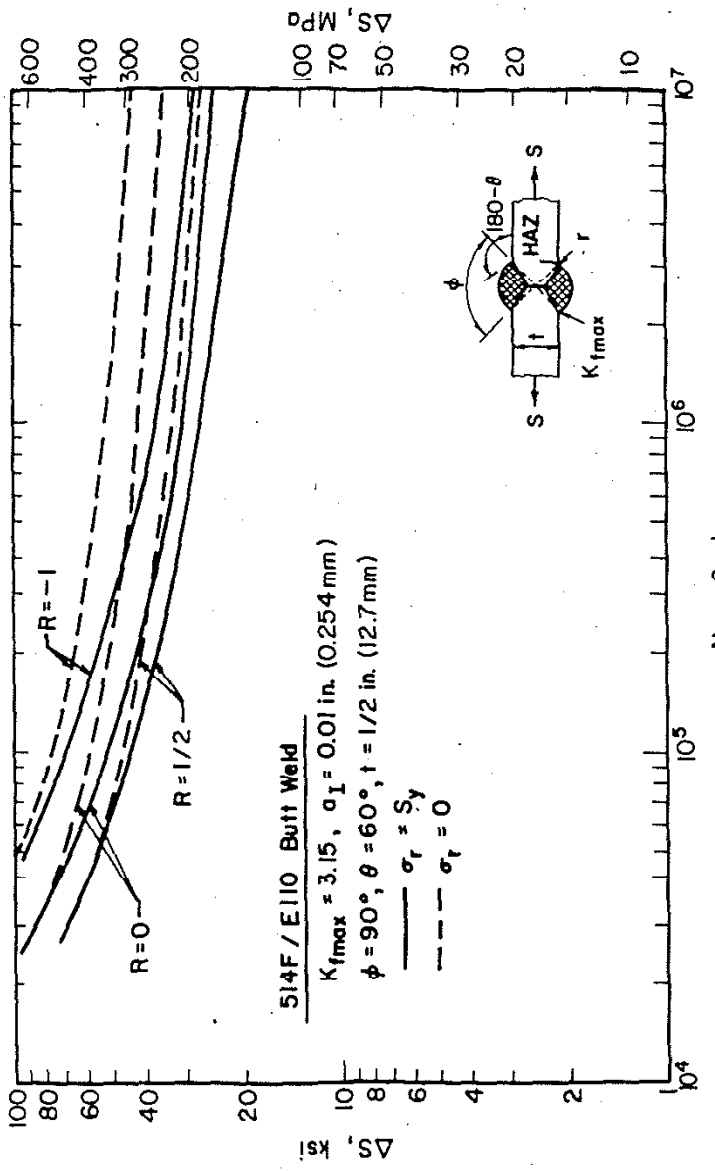

Figure 18. Predicted effect of weld-toe residual stress (σ_r = + S_y, 0) and stress ratio (R = -1, 0, + 1/2) on ASTM A514/E110 steel butt weldment fatigue life.

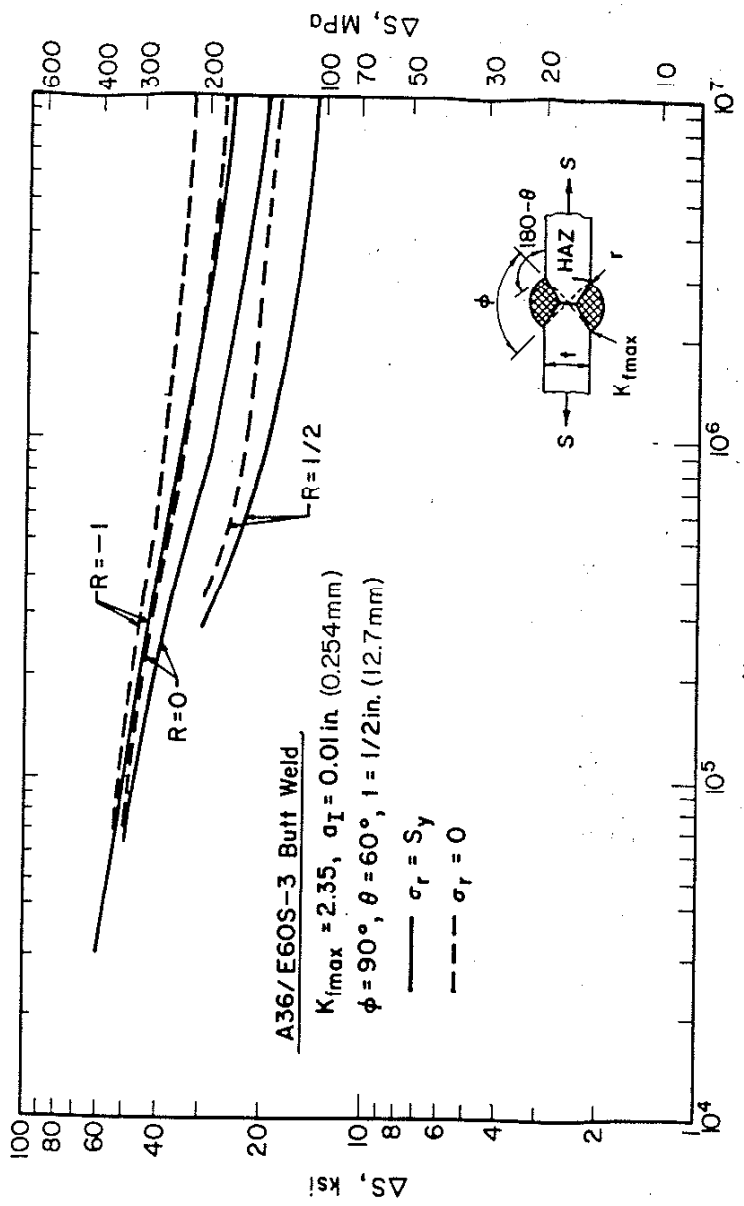

Figure 19. Predicted effect of weld-toe residual stress (σ_r = + S_y, 0), and stress ratio (R = -1, 0, + 1/2) on ASTM A36/E60S-3 steel butt weldment fatigue life.

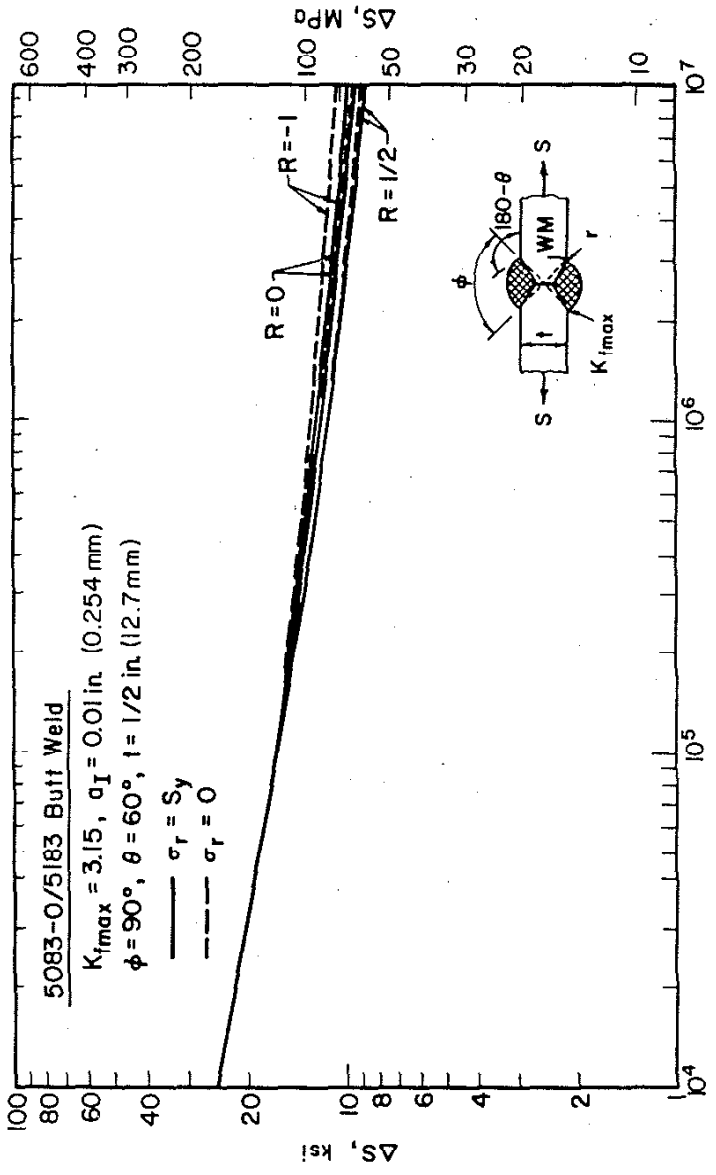

Figure 20. Predicted effect of weld-toe residual stress (σ_r = + S_y, 0) and stress ratio (R = -1, 0, 1/2) on 5083-O/5183 aluminum alloy butt weldment fatigue life.